Applied Mathematical Modelling 126 (2024) 698–712

Contents lists available at ScienceDirect

Applied Mathematical Modelling

journal homepage: www.elsevier.com/locate/apm

Maxwell homogenisation methodology for evaluation of effective elastic constants of weakly-nonlinear particulate composites

James Vidler [a], Andrei Kotousov [a,*], Ching-Tai Ng [b]

[a] The University of Adelaide, School of Electrical and Mechanical Engineering, Adelaide, Australia
[b] The University of Adelaide, School of Architecture and Civil Engineering, Adelaide, Australia

ARTICLE INFO

Keywords:
Maxwell's far-field methodology
Third order elastic constants
Homogenisation, finite strain
Nonlinear elasticity
Particulate composite

ABSTRACT

The far-field methodology, developed by J. C. Maxwell in 1873 for the evaluation of the electrical conductivity of a particle-reinforced material, is utilised to estimate the effective third order elastic constants of composite media containing a random distribution of spherical particles. The results are explicit analytical relationships derived using a perturbation solution, that are in a broad agreement with previous studies employing different homogenisation schemes. In contrast to other homogenisation schemes, Maxwell's methodology relies only on the far-field asymptotics. Therefore, the methodology may be more suitable for the evaluation of effective mechanical and physical properties of composites where the far-field asymptotics are known or can be derived. The main fundamental result of this work is the first demonstration that the Maxwell methodology may be applied to weakly nonlinear problems. Therefore, it can offer a new, simple method to analyse homogenisation problems in many other fields.

1. Introduction

The development of estimates of the effective properties of composite materials has a long history, and the assumptions and applicability of various homogenisation methods have been the discussed in many review papers [1]. One method for predicting the effective properties was proposed by J. C. Maxwell in 1873 [2] based on the far-field part of the mechanical response, and has subsequently been generalised to elastic media [3] and reformulated in terms of property contribution tensors and multipole expansions, allowing connections with other homogenisation methods to be established [4].

The far-field methodology of homogenisation was originally applied by Maxwell to estimate the effective electrical conductivity of a dispersion of spherical particles in an infinite medium with a different electric conductivity [2]. In deriving the effective conductivity, Maxwell calculated the perturbation in the electric far-field associated with a cluster of spheres embedded in an infinite medium with different electrical conductivity and suggested that the volume enclosing the cluster, treated as a single equivalent particle, produces an identical far-field perturbation as the cluster itself. It was also assumed that, in the far-field, the individual particles within the cluster may be treated as non-interacting, though it was suggested that this assumption is valid only for small particle concentrations. With these assumptions, a simple, closed-form expression for the overall electric conductivity of the composite medium was derived. Landauer [5] has provided the historical context of this development, which is also relevant to many other homogenisation problems including thermal conductivity, permittivity, magnetic permeability, and elasticity. The methodology de-

* Corresponding author.
E-mail address: andrei.kotousov@adelaide.edu.au (A. Kotousov).

https://doi.org/10.1016/j.apm.2023.11.002
Received 23 April 2023; Received in revised form 19 October 2023; Accepted 7 November 2023

Available online 17 November 2023

veloped by Maxwell has also been applied to the Eshelby solution [6], allowing the derivation of closed-form expressions for the effective linear elastic properties of composites with spheroidal-type inclusions [3,7,8]. These studies demonstrated the effectiveness and reliability of the estimates provided by the Maxwell methodology, which agree surprisingly well with experimental data and are in many cases identical to the results of more complex homogenisation methods [9–11]. It has also been observed that, despite Maxwell's original suggestion that the methodology should only be valid in the dilute case, the results remain reasonably accurate beyond low volume fractions. More recent applications of Maxwell's methodology have addressed the effects of imperfect interfaces [12,13], and extended the theory to viscoelastic media and to poroelasticity [14,15]. The latest studies have continued these efforts, with an additional focus on comparison with finite element models and other computational methods, e.g. the analysis of piezoelectric composites [16]; of initially-stressed media with imperfect interfaces between the constituents [17]; and in strain gradient elasticity [18].

The current study uses the Maxwell methodology to evaluate the third order elastic constants of nonlinear composites containing a random distribution of spherical particles. We assume that the composite is subjected to moderate deformations, and hence can be modelled as weakly-nonlinear. Such weakly-nonlinear materials are well-suited for modelling of metals, alloys and composite media loaded in the elastic regime, and are represented using the linear elastic constants as well as higher order elastic constants. In linear elasticity, the stress-strain response of a compressible and isotropic solid is described by two linear elastic constants, e.g. Lamé constants λ and μ. However, several experimentally observed phenomena, such as the influence of applied stress on the wave speed, commonly known as the acoustoelastic effect [19], may only be explained by consideration of the higher order elastic constants. The third order elastic constants (TOECs) arise naturally in the expansion of the elastic strain energy density function and are associated with the third order products of the strain components: in addition to the two linear elastic constants, a compressible hyperelastic solid possesses three independent TOECs [20]. Various equivalent representations of these constants exist, such as the Murnaghan constants l, m, n and the Landau-Lifshitz constants A, B, C. The TOECs reflect the lowest-order anharmonic response of an atomic lattice and play an important role in solid state physics. For example, TOECs often serve as a starting point for modelling the mechanical response under high strain levels, developing interatomic potentials, and studying behaviour of strained quantum wells. Since the TOECs are related to lattice properties, knowledge of them helps to study various phenomena in crystals, e.g. thermal expansion, Grüneisen's effect, interaction of thermal and acoustic phonons, and phase transitions. The effect of these nonlinear constants in most engineering applications is generally negligible and is disregarded in conventional stress analysis and structural integrity assessments. However, the TOECs play an important role in the evaluation of applied or residual stresses based on the acoustoelastic effect [21,22]. Other significant developments in the area of nondestructive damage evaluation (NDE) exploit the higher sensitivity of the TOECs (as compared with the linear elastic constants) to the accumulation of mechanical damage caused by fatigue, creep, radiation and impact in metals and composites [23–25]. In recognition of the importance of nonlinear effects, a framework has been developed to generalise the classical homogenisation methods of linear elasticity to account for nonlinear materials and finite deformations [26,27]. The resulting theory has been used to derive bounds and analytical solutions for several classes of incompressible and compressible composites [28]. Several recent studies focusing on incompressible composites have derived results for rigid inclusions [29,30] using the iterated dilute homogenisation method. The same approach has also been applied to porous incompressible materials considering both the elastic response [31] and the viscoelastic response [32]. The results for composites with compressible constituents are relatively sparse, though some recent investigations have used averaging theorems to derive estimates of the effective nonlinear properties [33–35].

Over the past two decades, the homogenisation of nonlinear composite materials has been the focus of many studies, often based on computational methods. These computational methods allow the analysis of complex geometries and finite deformations as well as modelling of nonlinear phenomena such as cavitation instabilities [36], the nonlinear properties of perforated plates [37], or damage caused by fracture of the reinforcement or matrix [38]. Recent studies have investigated approaches to reduce memory and storage requirements associated with these computational methods, for example by developing criteria for switching between appropriate finite element methods on the fly [39]. When the composite microstructure is periodic, the problem is greatly simplified by applying the numerical homogenisation approach, which provides a convenient and efficient method through the method of multiple scales [40]. The numerical homogenisation approach has been successfully extended to higher-order asymptotic homogenisation of hyperelastic and elastoplastic composites with periodic microstructure [41]; later, the same approach was extended to consider random microstructures [42]. However, the evaluation of the TOECs using numerical homogenisation methods poses a significant challenge. As mentioned before, for many classes of materials, the effect of the TOECs on the mechanical response may be indistinguishable from errors associated with discretisation, selection of the representative volume and other computational features. Moreover, the large number of independent elastic properties (ten in the case of two-phase compressible medium) suggest that a comprehensive parametric analysis is prohibitively difficult, and that an analytical approach would be most effective in solving this problem, particularly if this approach is based on Maxwell's methodology, which is relatively easy to apply in comparison with other homogenisation schemes.

In recognition of the growing interest in nonlinear phenomena as a means of identifying incipient structural damage in composite media [43] and of characterising the porosity during the processes of metal additive manufacturing [44], we apply Maxwell's methodology to a weakly nonlinear medium containing a distribution of spherical inhomogeneities. The results are simple analytical equations for the effective third order elastic constants the medium, which, in limiting cases, closely match results for incompressible media derived using different methods. The results are also the first demonstration that the Maxwell methodology may be generalised to nonlinear elastic media in the finite deformation regime and provides a foundation for future studies on the effective properties of other important composite geometries, such as fibre-reinforced composites.

This paper is organised as follows: a brief background of the finite deformation theory of elasticity, and the application of the Maxwell methodology applied to particulate composites are presented in section 2. In section 3 the second order elastic solution for a single inhomogeneity is briefly described and the far-field component needed for the Maxwell methodology is extracted. In section 4 the Maxwell homogenisation methodology is used to obtain closed-form expressions for the linear and nonlinear elastic properties of particulate composites. Section 5 compares the present solution to previous studies conducted using different homogenisation methodologies, including the special cases of a porous incompressible material and a dispersion of rigid fillers in an incompressible matrix, and a brief conclusion is presented in section 6.

2. Background

A brief summary of the governing equations of finite elasticity relevant to the Maxwell scheme is provided in the following section; full details may be found in standard references [45,46]. The deformation of a body with material points X and spatial points x may be described by the mapping φ. The gradient of the map φ is denoted $\boldsymbol{F}$, with components

$$F_A^a = \frac{\partial \varphi^a}{\partial X^A}$$

and the right Cauchy-Green deformation tensor is $\boldsymbol{C} = \boldsymbol{F}^T\boldsymbol{F}$. For a compressible hyperelastic isotropic material, a strain energy function W exists, and may be expressed as a function of I_1, I_2, I_3, the principal invariants of $\boldsymbol{C}$, where

$$I_1 = \mathrm{tr}(\boldsymbol{C}), \quad I_2 = \det \boldsymbol{C}\,\mathrm{tr}(\boldsymbol{C}^{-1}), \quad I_3 = \det \boldsymbol{C}.$$

In the case of a weakly nonlinear hyperelastic material, it is common to express the strain energy density function in Murnaghan's form [20], where

$$\begin{aligned} W(I_1,I_2,I_3) = {} & \tfrac{1}{8}(\lambda+2\mu)(I_1-3)^2 - \tfrac{1}{2}\mu(I_2-2I_1+3) + \tfrac{1}{24}(l+2m)(I_1-3)^3 - \tfrac{1}{4}m(I_1-3)(I_2-2I_1+3) \\ & + \tfrac{1}{8}n(I_1-I_2+I_3-1). \end{aligned} \tag{1}$$

The first Piola-Kirchhoff stress tensor, relating the traction in the spatial coordinates to the element of area in the material coordinates is related to W via

$$\boldsymbol{P} = \frac{\partial W}{\partial \boldsymbol{F}} \tag{2}$$

and, for elastostatic problems, must satisfy the equation of equilibrium

$$\mathrm{Div}\,\boldsymbol{P} = \boldsymbol{0} \tag{3}$$

where the divergence is taken with respect to the material coordinate system.

2.1. Maxwell's far-field methodology

In the context of elasticity, the averaging methodology proposed by Maxwell asserts that the effective elastic response of a composite medium consisting of a distribution of inhomogeneities may be estimated based on the far-field asymptotics of the stress/strain in the composite [2,4]. For a particulate composite consisting of a dispersion of spherical inhomogeneities, the far-field asymptotics may be estimated based on two equivalent models: (1) a cluster of inhomogeneities subjected to uniform displacement at infinity, where the interactions between inhomogeneities are assumed to be negligible in the far-field; and (2) a single, equivalent volume enclosing the cluster, with unknown elastic properties, and subjected to uniform displacement at infinity. The effective properties of the composite are those of the equivalent inhomogeneity, determined by equating the far-field components of each model.

The appropriate choice of the shape of the equivalent volume has been considered in several studies using both analytical and numerical methods [47,48]. It was found that the appropriate shape depends on the microstructural arrangement of the composite medium and the material symmetry of the particles: for anisotropic particles, the shape of the equivalent volume should be ellipsoidal, while a sphere is appropriate for randomly distributed isotropic particles. This study focuses on a random distribution of spherical inhomogeneities, and therefore a spherical geometry is considered in this study. Diagrams of the two models used in the Maxwell methodology are shown in Fig. 1.

In linear elasticity, the Maxwell methodology is applied to the far-field components of the linear stress/strain tensors. However, for the homogenisation of nonlinear elastic solids subjected to finite deformations, many distinct measures of stress and deformation are available. As discussed by Hill [26], it is desirable on physical grounds to select as macrovariables measures of stress and deformation for which the average over a referential volume is uniquely determined by the surface data. Hill [26] also demonstrated that the appropriate choices for elastic problems are the deformation gradient, $\boldsymbol{F}$, and the first Piola-Kirchhoff stress tensor, $\boldsymbol{P}$ [27]. Hence, we apply the Maxwell methodology to nonlinear elasticity by prescribing a uniform deformation gradient, $\overline{\boldsymbol{F}}$, at infinity and calculating the far-field asymptotics of $\boldsymbol{P}$ in the two equivalent models (Figs. 1b and 1c, respectively).

Due to Maxwell's assumption that the interaction between inhomogeneities is negligible in the far-field, the stress in a cluster consisting of N inhomogeneities may be expressed in the form

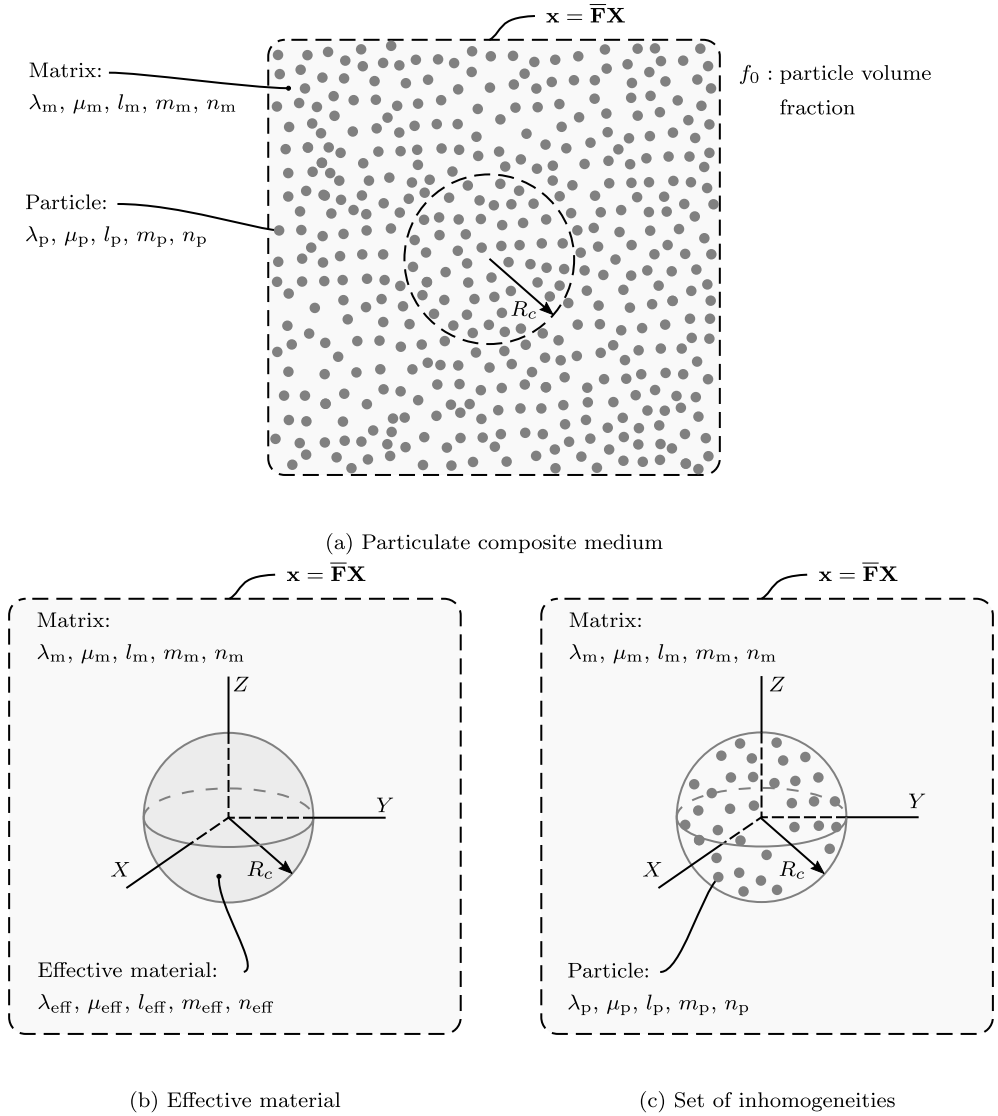

Fig. 1. The comparison materials for the Maxwell scheme for a prescribed boundary deformation $\overline{\boldsymbol{F}}$; (a) particulate composite medium; (b) a single inhomogeneity with material properties equal to the effective properties; and (c) cluster of inhomogeneities.

$$\sum_{i}^{N} \boldsymbol{P}^{(i)} = \boldsymbol{P}^{\infty} + \sum_{i}^{N} \widetilde{\boldsymbol{P}}^{(i)} \tag{4}$$

where $\boldsymbol{P}^{(i)}$ denotes the first Piola-Kirchhoff stress distribution in the i-th inhomogeneity. $\boldsymbol{P}^{\infty}$ is the uniform stress which would accompany $\overline{\boldsymbol{F}}$ if the medium were homogeneous, and is therefore known a priori. The terms $\widetilde{\boldsymbol{P}}^{(i)}$ represent the part of the stress which occurs due to the presence of each inhomogeneity. The far-field stress in the equivalent inhomogeneity may be expressed in the form

$$\boldsymbol{P}^{(\mathrm{eff})} = \boldsymbol{P}^{\infty} + \widetilde{\boldsymbol{P}}^{(\mathrm{eff})} \tag{5}$$

where $\boldsymbol{P}^{(\mathrm{eff})}$ is the stress distribution in Fig. 1b. The Maxwell methodology states that the far-field asymptotics of the stress distribution in each model are equal, so that the effective properties may be obtained by solving the equation

$$\widetilde{\boldsymbol{P}}^{(\mathrm{eff})} = \sum_{i}^{N} \widetilde{\boldsymbol{P}}^{(i)}. \tag{6}$$

If it is further assumed that all inhomogeneities have the same radii, then eq. (6) may be written in the form

$$\widetilde{\boldsymbol{P}}^{(\mathrm{eff})} = N\widetilde{\boldsymbol{P}} \tag{7}$$

or, in terms of the volume fraction of particles $f_0 = NV_p/V_c$, where V_p and V_c are, respectively, the volume of a single particle and the volume of the cluster,

$$\frac{1}{V_c}\widetilde{\boldsymbol{P}}^{(\mathrm{eff})} = \frac{f_0}{V_p}\widetilde{\boldsymbol{P}}. \tag{8}$$

Due to the random distribution of particles, and the assumption of non-interacting particles in the far-field, both the cluster and the equivalent inhomogeneity may be analysed based on the solution to a single elasticity problem. This problem is an isolated spherical inhomogeneity embedded in an infinite medium subjected to uniform displacement conditions at infinity and is the subject of the following section.

As mentioned, the following analysis relies upon the assumption that the interactions between particles are negligible in the far-field, which is not expected to be accurate for large volume fractions of inhomogeneities. However, within linear elasticity, the predicted effective properties have been observed to remain accurate for moderate volume fractions [3] and coincide with the lower Hashin-Shtrikman bounds. For these reasons, while the results of the present work are strictly only valid for low volume fractions, we compare the results at higher volume fractions to the results of other methods for certain limiting cases (e.g. incompressible materials, rigid fillers) in section 5 below. While such comparisons cannot be used to prove the accuracy of the present results for large concentrations of particles for general materials, they can provide indications of the errors involved in adopting the assumption of negligible interactions in the far-field. It should be noted that this assumption is not an essential component of the Maxwell methodology. Several studies have accounted for interactions by solving for the far-field of a cluster of inhomogeneities [4], though the results take the form of a computational solution, rather than the explicit analytical solution that is possible when the interactions are neglected.

3. Problem formulation and solution

The problem of an isolated spherical particle of radius R_i embedded in an infinite medium with different elastic properties may be formulated using the governing equations presented in section 2. We assume that both constituent materials are weakly nonlinear and described by eq. (1), where the elastic constants of the particle are $\lambda_p, \mu_p, l_p, m_p, n_p$ and those of the surrounding material are $\lambda_m, \mu_m, l_m, m_m, n_m$. As discussed in section 2.1, the boundary condition applied in the far-field is

$$\boldsymbol{x} = \overline{\boldsymbol{F}}\boldsymbol{X} \tag{9}$$

where the macroscopic deformation gradient may be expressed in terms of the macroscopic principal stretches $\overline{\lambda}_1, \overline{\lambda}_2, \overline{\lambda}_3$,

$$\overline{\boldsymbol{F}} = \mathrm{diag}(\overline{\lambda}_1, \overline{\lambda}_2, \overline{\lambda}_3). \tag{10}$$

3.1. Perturbation expansion

An exact solution to the nonlinear elasticity problem is not available for large deformations, though an approximate solution may be derived using a perturbation expansion [45,49]. Such perturbation expansions are common in the analysis of nonlinear elasticity problems, and are accurate provided that the perturbation parameter remains small. Applying the perturbation expansion to eqs. (2), (3) and (9), the displacement vector and first Piola-Kirchhoff stress tensor may be expanded as power series in the small parameter $U > 0$

$$\boldsymbol{u} = U\boldsymbol{u}_1 + U^2\boldsymbol{u}_2 + \dots \tag{11a}$$

$$\boldsymbol{P} = U\boldsymbol{P}_1 + U^2\boldsymbol{P}_2 + \dots \tag{11b}$$

where $U \ll 1$ is the magnitude of the displacement at infinity. The displacement vector and stress tensor associated with the linearised problem are $\boldsymbol{u}_1$ and $\boldsymbol{P}_1$, and $\boldsymbol{u}_2$ and $\boldsymbol{P}_2$ represent correction terms which establish equilibrium and satisfy the boundary conditions at second order. These corrections are determined using eqs. (2), (3) and (9). Using the perturbation expansion, the original nonlinear problem is reduced to a sequence of two linear problems with an approximation error of the order U^3. The first order terms in U constitute a standard linear elasticity problem, while the second order terms are equivalent to a linear elasticity problem with a body force: both problems may be solved using standard techniques developed for linear elasticity.

Provided that both constituents are isotropic, a composite medium containing a random distribution of spherical inhomogeneities is also isotropic on the macroscale, featuring only two independent effective linear elastic constants, and three independent effective TOECs. In this case, it is possible to determine all five effective elastic constants by considering an axisymmetric deformation, such that eq. (10) may be taken in the form $\overline{\boldsymbol{F}} = \mathrm{diag}(\overline{\lambda}_1, \overline{\lambda}_1, \overline{\lambda}_3)$.

As $\overline{\boldsymbol{F}}$ is axisymmetric, the linear displacement vector may be expressed in terms of the Papkovich-Neuber solution [50,51]. The linear displacement vector has the form

$$\boldsymbol{u}_1 = \frac{1}{2\mu}\nabla(\boldsymbol{X}\cdot\boldsymbol{b}_1 + \chi_1) - \frac{2(1-\nu)}{\mu}\boldsymbol{b}_1 \tag{12}$$

where $\boldsymbol{X}$ is the position vector from the origin, ν is the classical Poisson ratio, and $\boldsymbol{b}_1 = \eta_1 \mathbf{d}_Z$ with $\mathbf{d}_Z$ the unit vector aligned with the axis of symmetry of the deformation $\overline{\boldsymbol{F}}$. Then, to establish equilibrium, $\boldsymbol{b}_1$ and χ_1 must be harmonic functions, satisfying

$$\nabla^2 \boldsymbol{b}_1 = \mathbf{0}, \quad \nabla^2 \chi_1 = 0.$$

Explicit forms of $\boldsymbol{b}_1$ and χ_1 are provided in Appendix A. The corresponding linear elastic stress may be calculated using

$$\boldsymbol{P}_1(\boldsymbol{u}; \lambda, \mu) = \lambda(\mathrm{Div}\, \boldsymbol{u})\boldsymbol{G} + \mu[\mathrm{Grad}\, \boldsymbol{u} + \mathrm{Grad}\, \boldsymbol{u}^T] \tag{13}$$

where $\boldsymbol{G}$ is the second order identity tensor, and the divergence and gradient of are taken with respect to the material coordinates.

The second order problem features a body force, and therefore the displacement vector may be decomposed into the form $\boldsymbol{u}_2 = \boldsymbol{u}_2^{(h)} + \boldsymbol{u}_2'$ where $\boldsymbol{u}_2^{(h)}$ is solution corresponding to the homogeneous part of the second order problem, and $\boldsymbol{u}_2'$ is the particular solution associated with the body force. Due to axisymmetry,

$$\boldsymbol{u}_2^{(h)} = \frac{1}{2\mu}\nabla(\boldsymbol{X}\cdot\boldsymbol{b}_2 + \chi_2) - \frac{2(1-\nu)}{\mu}\boldsymbol{b}_2 \tag{14a}$$

$$\boldsymbol{u}_2' = \frac{1}{2\mu_m}\nabla\zeta^{(m)} - \frac{2(1-\nu_m)}{\mu_m}\nabla^2\boldsymbol{w}^{(m)} + \frac{1}{\mu_m}\nabla\mathrm{Div}\, \boldsymbol{w}^{(m)} \tag{14b}$$

where χ_2, $\boldsymbol{b}_2$ are harmonic functions, and ζ and $\boldsymbol{w}$ are a scalar and a vector function which are determined by $\boldsymbol{u}_1$. Further details of the second order terms are provided in Appendix A. The problem as formulated is lengthy, and many of the analytical manipulations are laborious, though they are standard in linear elasticity. Fortunately, the solution may be derived as a special case of a related solution [34]. Due to the nature of the Maxwell methodology, the calculation of the effective properties requires only the far-field parts, which are extracted in the following section.

3.2. Far-field solution

Having obtained the infinite medium solution, the far-field components of the stress distribution, eq. (7), may be calculated by taking the leading terms in the asymptotic expansion of the first Piola-Kirchhoff stress distribution, $\boldsymbol{P}$, $R \to \infty$. Omitting the constant stress $\boldsymbol{P}^\infty$, which is the uniform stress accompanying $\overline{\boldsymbol{F}}$, the leading term in the stress distribution is of order R^{-3} and all other terms may be neglected; for the displacement vector, the leading non-trivial term is of order R^{-2}. The far-field component of the displacement is $\widetilde{\boldsymbol{u}} = \widetilde{\boldsymbol{u}}^{(h)} + \widetilde{\boldsymbol{u}}'$, where

$$\widetilde{\boldsymbol{u}}^{(h)} = R_i^3\left[\frac{1}{2\mu}\nabla(\widetilde{\chi} + \boldsymbol{X}\cdot\widetilde{\boldsymbol{b}}) - \frac{2(1-\nu)}{\mu}\widetilde{\boldsymbol{b}}\right] \tag{15a}$$

$$\widetilde{\boldsymbol{u}}' = U^2 R_i^3\left[\frac{1}{2\mu_m}\nabla\widetilde{\zeta} + \widetilde{\boldsymbol{u}}_{\boldsymbol{w}}\right] \tag{15b}$$

and the potentials are

$$\widetilde{\chi} = (U F_0 R^{-1} + U^2 F_1 R^{-1}) P_0(\cos\Theta) \tag{16a}$$

$$\widetilde{\boldsymbol{b}} = (U G_1 R^{-2} + U^2 G_2 R^{-2}) P_1(\cos\Theta)\mathbf{d}_Z \tag{16b}$$

$$\widetilde{\zeta} = \frac{12\nu_m(\lambda_m + 3\mu_m + 2m_m)}{35(\lambda_m + \mu_m)}\left[3A_2 - 2(1-2\nu_m)B_1\right] G_1 \tag{16c}$$

$$\widetilde{\boldsymbol{u}}_{\boldsymbol{w}} = \left[(3-4\nu_m)a_1 R^{-2} P_2(\cos\Theta) + a_2 R^{-2} P_4(\cos\Theta)\right]\mathbf{d}_R - \left[(1-2\nu_m)a_1 R^{-2} P_2'(\cos\Theta)\right]\mathbf{d}_\Theta \tag{16d}$$

with a_1, a_2 provided in Appendix B. The far-field stress $\widetilde{\boldsymbol{P}}$ may be decomposed into the form

$$\widetilde{\boldsymbol{P}} = \boldsymbol{P}_1(\widetilde{\boldsymbol{u}}; \lambda_m, \mu_m) + U^2\widetilde{\boldsymbol{P}}'(\boldsymbol{u}_1) \tag{17}$$

where the first term arises from eq. (13), the linear form of the stress-displacement relation, applied to $\widetilde{\boldsymbol{u}}$, and the second term represents the effect of finite deformation associated with $\boldsymbol{u}_1$, presented in full in Appendix B. Finally, the far-field stress may be expressed in the form of a perturbation expansion in U,

$$\widetilde{\boldsymbol{P}} = U\widetilde{\mathbf{P}}^{(1)} + U^2\widetilde{\boldsymbol{P}}^{(2)}. \tag{18}$$

Using the procedure described above, explicit expressions for $\widetilde{\boldsymbol{P}}$ may be derived for certain simple deformations. If the deformation is infinitesimally incompressible with $\overline{\lambda}_1 = \overline{\lambda}_2 = 1 - \frac{1}{2}U$ and $\overline{\lambda}_3 = 1 + U$, the non-zero components of $\widetilde{\boldsymbol{P}}^{(1)}$ with respect to a spherical basis are

$$\widetilde{P}_{11}^{(1)} = (9K_m + 8\mu_m)(1 + 3\cos 2\Theta)p_i \tag{19a}$$

$$\widetilde{P}_{22}^{(1)} = -\mu_m(5 + 3\cos 2\Theta)p_i \tag{19b}$$

$$\widetilde{P}_{33}^{(1)} = \mu_m(1 - 9\cos 2\Theta)p_i \tag{19c}$$

$$\widetilde{P}^{(1)}_{12} = \widetilde{P}^{(1)}_{21} = 9K_m \sin 2\Theta p_i \tag{19d}$$

where

$$p_i = \frac{5\mu_m(\mu_p - \mu_m)}{2[\mu_m(9K_m + 8\mu_m) + 6\mu_p(K_m + 2\mu_m)]} \left(\frac{R_i}{R}\right)^3.$$

If the deformation is spherically-symmetric, i.e. $\overline{\lambda}_1 = \overline{\lambda}_2 = \overline{\lambda}_3$, the radial normal component of $\widetilde{\boldsymbol{P}}^{(1)}$ is

$$\widetilde{P}^{(1)}_{11} = \left(\frac{R_i}{R}\right)^3 \frac{12\mu_m(K_p - K_m)}{3K_p + 4\mu_m} \tag{20}$$

with $\widetilde{P}^{(1)}_{22} = \widetilde{P}^{(1)}_{33} = -\frac{1}{2}\widetilde{P}^{(1)}_{11}$ and all other components zero.

In most cases, the second order part of $\widetilde{\boldsymbol{P}}^{(2)}$ is extremely lengthy. However, the results are relatively simple for a spherically-symmetric deformation. The radial normal stress in this case is

$$\begin{aligned}\widetilde{P}^{(2)}_{11} = \left(\frac{R_i}{R}\right)^3 \Bigg[&\frac{18(K_p - K_m)}{(3K_m + 4\mu_m)(3K_p + 4\mu_m)^3} p_s + \frac{36\mu_m(3K_m + 4\mu_m)^2}{(3K_p + 4\mu_m)^3}(l_p + \tfrac{1}{9}n_p) - \frac{36\mu_m}{3K_p + 4\mu_m}(l_m + \tfrac{1}{9}n_m) \\ &+ \frac{108(K_p - K_m)[(3K_m + 4\mu_m)K_p + 2\mu_m(K_p - K_m)]}{(3K_m + 4\mu_m)(3K_p + 4\mu_m)^2}(m_m - \tfrac{1}{6}n_m) - \frac{108\mu_m(K_p - K_m)^3}{(3K_m + 4\mu_m)(3K_p + 4\mu_m)^3} n_m \Bigg]\end{aligned} \tag{21}$$

where

$$\begin{aligned}p_s = &(3K_m + 4\mu_m)^2(3K_m^2 + K_m\mu_m + 4\mu_m^2) + (K_p - K_m)^2(27K_m^2 + 90K_m\mu_m + 90\mu_m^2) \\ &+ 3(K_p - K_m)(3K_m + 4\mu_m)(6K_m^2 + 11K_m\mu_m + 8\mu_m^2)\end{aligned}$$

with $\widetilde{P}^{(2)}_{22} = \widetilde{P}^{(2)}_{33} = -\frac{1}{2}\widetilde{P}^{(2)}_{11}$ and all other components zero. The far-field stress tensor for other deformations may be expressed similarly, using the solution derived in section 3.1.

4. Effective elastic constants

As discussed in section 2.1, the Maxwell methodology uses the far-field stress in two different models to calculate the effective properties of a composite medium, via eq. (7), reproduced here:

$$\widetilde{\boldsymbol{P}}^{(\mathrm{eff})} = N\widetilde{\boldsymbol{P}}$$

where $\widetilde{\boldsymbol{P}}^{(\mathrm{eff})}$ is the far-field stress in the equivalent single inhomogeneity, and $\widetilde{\boldsymbol{P}}$ is the far-field stress in the cluster of N inhomogeneities. For a composite medium containing spherical particles, the effective linear elastic constants K_{eff}, μ_{eff}, and the effective TOECs l_{eff}, m_{eff}, n_{eff} may be derived using the expressions for the far-field stress $\widetilde{\boldsymbol{P}}$ presented in section 3.2.

4.1. Linear elastic constants

The effective bulk modulus may be obtained from the result for a spherically-symmetric motion; in the equivalent single inhomogeneity, Fig. 1b, the far-field stress is obtained from eq. (20) with the modifications $R_i \to R_c$, $K_p \to K_{\mathrm{eff}}$, such that the far-field perturbation is

$$\left(\frac{R_c}{R}\right)^3 \frac{12\mu_m(K_{\mathrm{eff}} - K_m)}{3K_{\mathrm{eff}} + 4\mu_m}$$

Hence, eq. (7) provides

$$\left(\frac{R_c}{R}\right)^3 \frac{12\mu_m(K_{\mathrm{eff}} - K_m)}{3K_{\mathrm{eff}} + 4\mu_m} = N\left(\frac{R_i}{R}\right)^3 \frac{12\mu_m(K_p - K_m)}{3K_p + 4\mu_m}.$$

After simplification and use of the relation $f_0 = NR_i^3/R_c^3$, where f_0 is the volume fraction of particles, the above equation provides the effective bulk modulus,

$$K_{\mathrm{eff}} = \frac{K_m(3K_p + 4\mu_m) + 4f_0\mu_m(K_p - K_m)}{3K_p + 4\mu_m - 3f_0(K_p - K_m)}. \tag{22}$$

Similarly, for the far-field stress corresponding to an infinitesimal incompressible deformation, eq. (19), the Maxwell methodology provides

$$\frac{\mu_{\mathrm{eff}} - \mu_m}{\mu_m(9K_m + 8\mu_m) + 6\mu_{\mathrm{eff}}(K_m + 2\mu_m)} = f_0 \frac{\mu_p - \mu_m}{\mu_m(9K_m + 8\mu_m) + 6\mu_p(K_m + 2\mu_m)}$$

which may be solved for μ_{eff} to provide the effective shear modulus

$$\mu_{\text{eff}} = \mu_m \frac{6\mu_p(K_m + 2\mu_m) + (9K_m + 8\mu_m)[(1-f_0)\mu_m + f_0\mu_p]}{\mu_m(9K_m + 8\mu_m) + 6(K_m + 2\mu_m)[f_0\mu_m + (1-f_0)\mu_p]}. \tag{23}$$

As is to be expected, the effective linear elastic constants eqs. (22) and (23) reproduce results derived using the Maxwell methodology in a previous study, [3, Eqs. (3.19) and (4.17)]. The results are also identical to those derived by Kerner using a different methodology, [52, Eqs. (5) and (8)]; as well as the results of the Mori-Tanaka method, [53, Eq. (6.2)].

4.2. Third order elastic constants

The effective TOECs may be calculated using the nonlinear part of eq. (7). Substantial simplifications of the results occur if, instead of Murnaghan's form l, m, n, the TOECs are expressed in terms of the Murnaghan constant n and the linear combinations $q = l + \frac{1}{9}n$ and $s = m - \frac{1}{6}n$. Repetition of the process described in section 4.1 but applied to the second order terms in far-field stress (e.g. eq. (21) for a spherically-symmetric deformation) provides the effective TOECs predicted by the Maxwell methodology,

$$\begin{aligned} q_{\text{eff}} = {} & \frac{(1-f_0)(3K_p + 4\mu_m)^3}{h^3} q_m + \frac{f_0(3K_m + 4\mu_m)^3}{h^3} q_p + \frac{18f_0(1-f_0)(K_p - K_m)^2(3K_p + 4\mu_m)}{h^3} s_m \\ & + \frac{3f_0(1-f_0^2)(K_p - K_m)^3}{h^3} n_m + \frac{27f_0(1-f_0)(K_p - K_m)^2\left[K_m(3K_p + 2\mu_m) - 2\mu(f_0K_m + (1+f_0)K_p)\right]}{2h^3} \end{aligned} \tag{24a}$$

$$\begin{aligned} s_{\text{eff}} = {} & \frac{1-f_0}{hk^2} p_3 s_m + \frac{25f_0\mu_m^2(3K_m + 4\mu_m)^3}{hk^2} s_p + \frac{120f_0(1-f_0)\mu_m^2(3K_p + 4\mu_m)(\mu_p - \mu_m)^2}{hk^2} q_m \\ & + \frac{f_0(1-f_0)(K_p - K_m)(\mu_p - \mu_m)}{2hk^2} p_1 n_m + \frac{2f_0(1-f_0)(\mu_p - \mu_m)}{hk^2} p_2 \end{aligned} \tag{24b}$$

$$\begin{aligned} n_{\text{eff}} = {} & \frac{1-f_0}{7k^3} p_5 n_m + \frac{125f_0\mu_m^3(3K_m + 4\mu_m)^3}{k^3} n_p + \frac{7200f_0(1-f_0^2)\mu_m^3(\mu_p - \mu_m)^3}{7k^3} q_m + \frac{180f_0(1-f_0)\mu_m(\mu_p - \mu_m)^2}{7k^3} p_1 s_m \\ & - \frac{60f_0(1-f_0)\mu_m(\mu_p - \mu_m)^2}{7k^3} p_4 \end{aligned} \tag{24c}$$

where

$$h = 4\mu_m + 3[f_0K_m + (1-f_0)K_p], \quad k = \mu_m(9K_m + 8\mu_m) + 6(K_m + 2\mu_m)[f_0\mu_m + (1-f_0)\mu_p] \tag{25}$$

and the constants p_1, p_2, p_3, p_4 and p_5 are parameters depending on the linear elastic constants and f_0, presented in Appendix C. It may be observed that the use of q, s and n reduces the number of independent parameters in each effective TOEC (i.e. q_{eff} does not depend on s_p or n_p, s_{eff} does not depend on q_p or n_p, and n_{eff} does not depend on q_p or s_p). Additionally, the three effective TOECs in eq. (24) may be substituted back into eq. (7) to demonstrate that these effective elastic constants satisfy the governing equations of the Maxwell methodology for any axisymmetric deformation at second order.

It may be observed that the Maxwell methodology expression for q_{eff} is identical to the prediction based on the referential volume averaging methodology presented in [34, Eq. (34)], though the other TOECs differ. When restricted to a dilute distribution (i.e. first order power series in f_0 about $f_0 = 0$) the Maxwell methodology provides results that are identical to those of the volume averaging methodology presented in [54, Eq. (42)] and [34, Eq. (35)]. A detailed discussion of the Maxwell methodology in comparison to other results is the subject of the following section.

5. Comparisons with previous studies

One of the most important applications of the present results is to modelling and prediction of damage evolution. For example, the results for compressible constituents may be readily adapted to consider a compressible matrix containing a distribution of spherical voids. For ductile materials, particularly structural metals and alloys, the presence of voids is strongly linked to the state of damage of the structure, and the process of damage accumulation has been associated with the growth and coalescence of these voids [55,56].

For incompressible materials, the model of an incompressible matrix containing pores has attracted substantial attention for its role in prediction of cavitation in elastomers, which has been shown to be a significant mechanism in the development of damage [57]. Incompressible materials with rigid inclusions have also been used to predict the stiffness enhancement associated with the addition of rigid fillers to elastomeric materials [29,30]. Finally, large deformation failure modelling of polymer syntactic foams, which are common in marine and aerospace applications [58], has been undertaken based on incompressible materials containing a combination of vacuous pores and rigid fillers, depending on the fracture/buckling response of constituent particles [38].

The effective linear elastic constants and TOECs derived in section 4 may be used to derive results for several specific cases of physical interest, including incompressible materials, materials featuring a distribution of voids, and materials featuring rigid inclusions. The appropriate limits needed to specialise compressible results to these cases, and the effective properties in each case, are presented in the following subsections. Comparison of the estimates of the Maxwell methodology with the results of other approaches is undertaken in each subsection. Specifically, we compare our results to: the effective properties derived via averaging of the strain energy; and results for incompressible materials derived using the iterated dilute homogenisation methodology.

5.1. Compressible matrix, compressible particle

The Maxwell methodology results may be compared with the estimates of the TOECs provided by [33, Eq. (46)], which were derived by averaging the strain energy at second order using Eshelby's linear elastic solution for a spherical inhomogeneity in combination with a careful use of integral transformations. The results were validated against Finite Element simulations for a range of material property contrasts, and an excellent agreement was observed in almost all cases for volume fractions up to $f_0 = 0.2$. The differences between the results of the Maxwell scheme, eq. (24) and the corresponding effective elastic constants of [33] (denoted here q_W, s_W, n_W) are

$$q_W - q_{\text{eff}} = -\frac{f_0^2(1-f_0)}{h^3}(9\mu_m + 3n_m)(K_p - K_m)^3 \tag{26a}$$

$$s_W - s_{\text{eff}} = -\frac{6f_0^2(1-f_0)\mu_m^2}{hk^2}\Delta_s(K_p - K_m)(\mu_p - \mu_m)^2 \tag{26b}$$

$$n_W - n_{\text{eff}} = -\frac{4f_0^2(1-f_0)\mu^2}{7k^3}\Delta_n(\mu_p - \mu_m)^3 \tag{26c}$$

where h, k are given by eq. (25), and

$$\Delta_s = \frac{35 - 72\nu_m + 40\nu_m^2}{(1-2\nu_m)^2}\mu_m + \frac{2(13-20\nu_m)}{1-2\nu_m}s_m - \frac{2 - 8\nu_m + 5\nu_m^2}{(1-2\nu_m)^2}n_m$$

$$\Delta_n = 1800q_m - \frac{540(2 - 8\nu_m + 5\nu_m^2)}{(1-2\nu_m)^2}s_m + \frac{443 - 2460\nu_m + 4065\nu_m^2 - 2050\nu_m^3}{(1-2\nu_m)^3}n_m - \frac{6(241 - 1710\nu_m + 2670\nu_m^2 - 1400\nu_m^3)}{(1-2\nu_m)^3}\mu_m.$$

It may be observed that the differences in eq. (26) are independent of the TOECs of the particle phase (though they do depend on K_p and μ_p) and the two methodologies are also identical up to first order in f_0. Furthermore, numerical investigations reveal that, for physically reasonable values of the elastic properties, the error terms are minor in comparison with the other terms, usually only becoming significant at high volume fractions, a condition which violates the assumptions involved in both methodologies.

5.2. Incompressible materials

The results derived for compressible materials in section 4.2 may be adapted to incompressible materials using the incompressible limits provided by [59], which have the form

$$(1-2\nu)B \to -\mu, \quad (1-2\nu)^3 C \to 0 \tag{27}$$

where $A = n$, $B = m - \frac{1}{2}n$, and $C = l - m + \frac{1}{2}n$ are the Landau-Lifshitz constants. Applying these limits to eq. (1) leads to the third order incompressible strain energy function

$$W_{\text{I},3} = \mu \operatorname{tr}\boldsymbol{E}^2 + \frac{1}{3}A \operatorname{tr}\boldsymbol{E}^3 \tag{28}$$

which is equivalent, up to third order in the products of the strain, to the Mooney-Rivlin incompressible material model [59]. When $A = -4\mu$ in eq. (28), the neo-Hookean strain energy function is recovered,

$$W = \frac{1}{2}\mu(I_1 - 3). \tag{29}$$

5.2.1. Incompressible matrix containing voids

Using the limits for a distribution of voids

$$\lambda_p \to 0, \quad \mu_p \to 0, \quad l_p \to 0, \quad m_p \to 0, \quad n_p \to 0$$

in conjunction with eq. (27), the effective properties of a neo-Hookean matrix containing a distribution of voids may be derived. The effective elastic constants are

$$\mu_{\text{eff}}/\mu = \frac{(1-f_0)}{1 + \frac{2}{3}f_0} \tag{30a}$$

$$K_{\text{eff}}/\mu = \frac{4(1-f_0)}{3f_0} \tag{30b}$$

$$A_{\text{eff}}/\mu = -\frac{4(1-f_0)(1 + \frac{232}{189}f_0 + \frac{79}{189}f_0^2)}{(1 + \frac{2}{3}f_0)^3} \tag{30c}$$

$$(1-2\nu_{\text{eff}})B_{\text{eff}}/\mu = -\frac{(1-f_0)(1 + \frac{210}{189}f_0 + \frac{55}{189}f_0^2 - \frac{9}{189}f_0^3)}{(1 + \frac{2}{3}f_0)^3(1 + \frac{11}{12}f_0)} \tag{30d}$$

$$(1-2\nu_{\text{eff}})^3 C_{\text{eff}}/\mu = -\frac{33f_0(1-f_0)(1+\frac{315}{231}f_0+\frac{154}{231}f_0^2+\frac{32}{231}f_0^3+\frac{8}{231}f_0^4)}{64(1+\frac{2}{3}f_0)^3(1+\frac{11}{12}f_0)^3} \tag{30e}$$

where μ denotes the shear modulus of the neo-Hookean matrix. Note that the composite medium exhibits macroscopic compressibility due to the presence of the pores, as found in ref. [60].

Comparison may be made with ref. [31, Eq. (13)], where an analytical result for the effective strain energy density function for a neo-Hookean material containing a distribution of voids subjected to spherically-symmetric deformations was presented. It is straightforward to show that if the deformation is spherically-symmetric, then the volume-averaged deformation gradient has the form $\overline{\mathbf{F}} = \text{diag}(\overline{J}^{1/3}, \overline{J}^{1/3}, \overline{J}^{1/3})$, and eq. (30) may be used to show that the effective strain energy function is

$$\overline{W} = \mu\left[\frac{3(1-f_0)}{2f_0}(\overline{J}^{2/3}-1)^2 - \frac{(1-f_0)(11+5f_0)}{8f_0^2}(\overline{J}^{2/3}-1)^3\right] \tag{31}$$

which is identical, up to third order in $\overline{J}-1$, to the effective strain energy function for spherically-symmetric deformations presented in [31, Eq. (13)]. Note that the results of the method presented in [33] do not reproduce the results of [31], due to the use of different assumptions in that study.

5.2.2. Rigid inclusions

For an incompressible neo-Hookean matrix containing a distribution of rigid inclusions, the effective elastic constants are calculated using eq. (27) in conjunction with

$$\mu_m/\mu_p \to 0, \quad A_m/A_p \to 0.$$

The overall response is incompressible, with the effective elastic constants

$$\mu_{\text{eff}}/\mu = \frac{1+\frac{3}{2}f_0}{1-f_0} \tag{32a}$$

$$A_{\text{eff}}/\mu = -\frac{4+\frac{79}{14}f_0}{1-f_0} \tag{32b}$$

where μ denotes the shear modulus of the neo-Hookean matrix. Applying a first order Taylor expansion in f_0 about $f_0 = 0$ of eq. (32) provides

$$\mu_{\text{eff}}/\mu = 1+\tfrac{5}{2}f_0 \tag{33a}$$

$$A_{\text{eff}}/\mu = -4-\tfrac{135}{14}f_0. \tag{33b}$$

Note that, as expected, eq. (33a) is identical to a previously-published result in linear elasticity, [61, Eq. (12)], and the first order expansion in f_0 of the effective strain energy function for infinitesimal deformations is

$$\overline{W}_{\text{inf}}/\mu = \frac{1}{2}(\overline{I}_1-3) + f_0\left[\frac{145}{112}(\overline{I}_1-3) - \frac{5}{112}(\overline{I}_2-3)\right]f_0$$

which is identical to the linear elasticity result presented in [29, Eq. (46)].

Turning to larger values of f_0, the Maxwell methodology prediction for the effective strain energy function of the composite medium, from eq. (32), is

$$\overline{W}/\mu = \frac{1}{2(1-f_0)}(\overline{I}_1-3) + \frac{89f_0}{112(1-f_0)}(\overline{I}_1-3) - \frac{5f_0}{112(1-f_0)}(\overline{I}_2-3). \tag{34}$$

The effective response of a suspension of rigid inclusions in a neo-Hookean matrix subjected to large deformations has been investigated in prior studies using both analytical and computational methods [29,30]. Though the present results are restricted to small deformations, comparison with those results can constitute a limited form of validation. In those studies it was observed that, for both small and large deformations, the dependence of $\overline{W}$ on $\overline{I}_2 - 3$ was weak, which is supported by eq. (34), where the corresponding coefficient is significantly smaller than the other terms.

Similarly, eq. (34) may be compared to the analytical prediction derived using the iterated dilute homogenisation method [30], which was found to be substantially in agreement with finite element results. Additionally, the finite element results were relatively insensitive to the size of the particle phase. The results may be compared in terms of the macroscopic first Piola-Kirchhoff stress tensor for several loading conditions: (i) uniaxial extension, $\overline{P}_{\text{un}}$, (ii) pure shear, $\overline{P}_{\text{ps}}$, and (iii) simple shear, $\overline{P}_{\text{ss}}$; for which the equations in terms of $\overline{W}$ are presented in [30, Eqs. (68–70)]. The predictions of the macroscopic stress for each loading condition across a wide range of deformations are shown in Fig. 2. For the case of $f_0 = 0.05$, the results of the Maxwell methodology are almost indistinguishable from those of [30]; the differences increase with the magnitude of the deformation, and with the increase in the volume fraction f_0. For larger values of the volume fraction, the results of the Maxwell scheme appear to be accurate only for small-to-moderate values of the applied stretch. This result is interesting, as it indicates that, for neo-Hookean materials with rigid fillers at least, the Maxwell scheme serves as a good approximation despite neglecting particle interactions in the far-field.

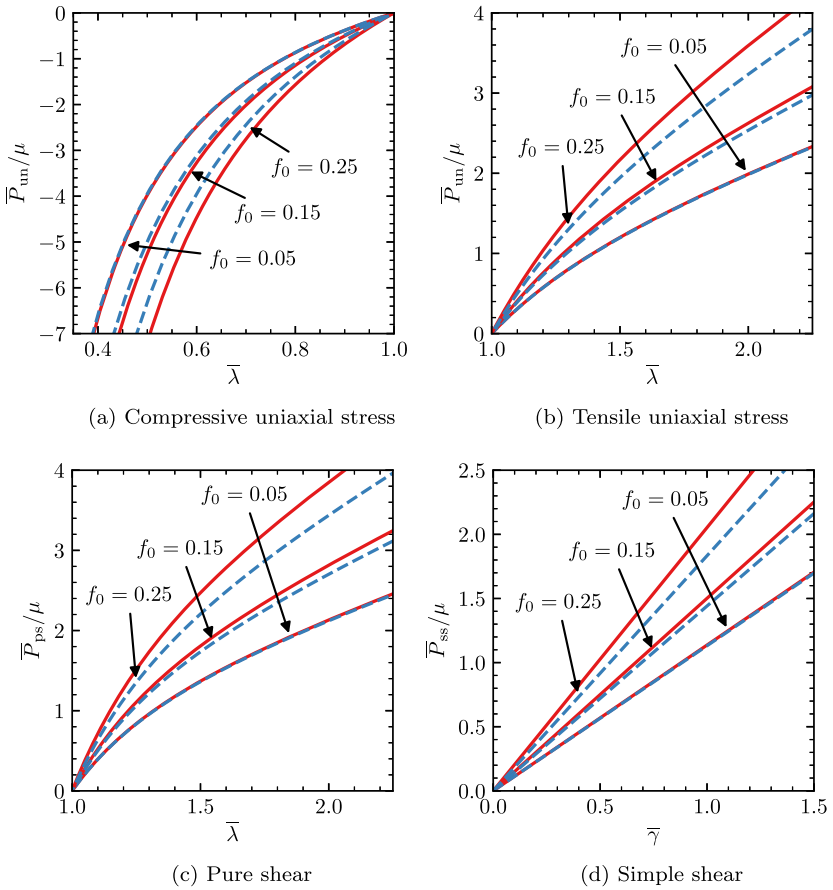

Fig. 2. Macroscopic stress components for neo-Hookean rubber reinforced by rigid inclusions for (a) uniaxial compression, (b) uniaxial tension, (c) pure shear, and (d) simple shear. In (a), (b) and (c) the applied macroscopic stretch is denoted $\overline{\lambda}$; in (d) the applied macroscopic shear is denoted $\overline{\gamma}$. The solid red line corresponds to the iterated dilute homogenisation methodology [30]; the broken blue line to the Maxwell methodology.

In general, it can be observed that the macroscopic response for a neo-Hookean composite with rigid fillers predicted by the Maxwell scheme is moderately accurate for small as well as large deformations, provided that the volume fraction of inhomogeneities remains low. This unexpected phenomenon, where results derived using a perturbation expansion remain approximately valid for large deformations is interesting and opens up avenues for further investigation of other types of nonlinear composite media using the perturbation method.

6. Conclusion

Since its original formulation by Maxwell in the 1870s, the far-field homogenisation methodology has been successfully utilised in many applications, and even reinvented in some research areas, e.g. in early works on thermoelasticity. One reason behind the long-term success of the methodology is its simplicity, which allows the derivation of analytical, closed-form expressions for the effective properties based on the far-field solutions to two problems: the first is a finite cluster of inhomogeneities embedded in an infinite medium; and the second a single equivalent inhomogeneity with unknown properties. In general, the selection of the shape of the equivalent inhomogeneity is not clearly defined in the Maxwell methodology. However, in the case of random microstructure the effective properties are isotropic, which dictates the selection of a spherical shape for the equivalent inhomogeneity. It was demonstrated for linear elastic materials that the relationships derived using the Maxwell methodology obey strict variational bounds and are often identical or very close to those obtained with more established and more complex homogenisation methodologies [62].

Many recent studies have worked to rigorously justify the application of the Maxwell methodology to linear elasticity by establishing connections with the concepts of multipole expansions and property contribution tensors, shedding light on why identical or almost identical results can be obtained using the much simpler analysis based on Maxwell's formulation [4]. Though the methodology was first applied to estimate the effective electric conductivity of a particulate composite, its further development has been largely driven by linear elasticity problems associated with finding the elastic constants of multiphase composites. Some of the latest theoretical developments apply the methodology to composites with imperfect interfaces, and to viscoelastic materials; and new applications of this elegant methodology are fast expanding.

In this work we applied Maxwell's methodology to nonlinear elastic materials and obtained explicit analytical expressions for the effective third order elastic constants of composite media containing a random distribution of spherical particles. This type of composite material has been extensively-investigated in recent studies using several other homogenisation methodologies [33,34], and therefore represents an ideal test case for the generalisation of the Maxwell methodology to nonlinear materials subjected to finite deformations. The present derivation used a perturbation solution for an isolated spherical inhomogeneity to derive results for the Maxwell methodology; the derived equations are very similar to the results presented by Semenov and Beltukov [33]. The latter results have been shown to agree well with FE simulations over a wide range of macroscopic deformations and material properties for the constituents. Additionally, within the accuracy of the perturbation method, the application of the present results to an incompressible porous material match exactly the solutions presented by Hashin [60] and by Shrimali et al. [31] for a spherically-symmetric macroscopic deformation. Moreover, for an incompressible matrix containing a distribution of rigid fillers, the present relationships agree quite well with analytical studies based on the iterated dilute homogenisation method and associated FE results [29,30], even for moderately large deformations.

Based on the comparisons presented in section 5 of this article, it may be concluded that Maxwell's methodology is applicable to the estimation of the effective elastic constants of a compressible medium containing a dispersion of spherical particles in both linear elasticity and weakly-nonlinear elasticity. Furthermore, comparisons with large deformation results for incompressible materials suggests that the Maxwell methodology may also be reliable for nonlinear materials subjected to large deformations, though further investigation is needed for confirmation. One of the advantages of the Maxwell methodology is that it only requires the far-field components of the stress, and hence it may be applicable to a different and possibly wider class of problems than other homogenisation methodologies (i.e. there may be some composites for which the far-field stress is easier to derive than the quantities needed for other methodologies).

The new fundamental result of this work is the demonstration that the Maxwell methodology can be successfully extended to weakly nonlinear problems. This result offers a new approach to analyse similar homogenisation problems in various fields of mechanics and physics e.g. thermal conductivity and expansion, magnetic permeability and diffusion. Future extensions to this study could consider ellipsoidal inhomogeneities, which would expand the applicability of the results to anisotropic composites, such as fibre reinforced composites, or composites containing spheroidal particles, though deriving the second order elastic solution for these cases is anticipated to be extremely challenging. In addition to use of the present results as a benchmark for numerical solutions, the recent developments of Maxwell-based computational methods in linear elasticity may also be considered in the context of nonlinear materials subjected to finite deformations. The advantages of these methods include direct applicability to in-situ experimental measurements, as discussed in [63,64].

Declaration of competing interest

The authors declare that they have no known competing financial interests or personal relationships that could have appeared to influence the work reported in this paper.

Data availability

Data will be made available on request.

Funding

This research was partially supported by the Australian Government through the Australian Research Council's Discovery Projects funding scheme (project DP200102300); and the Australian Government Research Training Program (RTP) Scholarship.

Appendix A. Elastic solution potentials

The details of the linear and second order displacement solution for a single spherical inhomogeneity of radius R_i embedded in an unbounded medium are summarised in this section. For $R > R_i$, the harmonic functions in eqs. (12) and (14) are given by the expressions

$$\chi_1 = F_0 R_i^3 R^{-1} + (A_2 R^2 + F_2 R_i^5 R^{-3}) P_2(\cos\Theta) \tag{A.1a}$$

$$\eta_1 = (B_1 R + G_1 R_i^3 R^{-2}) P_1(\cos\Theta) \tag{A.1b}$$

$$\chi_2 = F_1 R_i^3 R^{-1} + F_3 R_i^5 R^{-3} P_2(\cos\Theta) + F_5 R_i^7 R^{-5} P_4(\cos\Theta) \tag{A.1c}$$

$$\eta_2 = G_2 R_i^3 R^{-2} P_1(\cos\Theta) + G_4 R_i^5 R^{-4} P_3(\cos\Theta) \tag{A.1d}$$

and for $R < R_i$,

$$\chi_1 = A_2^{(p)} R^2 P_2(\cos\Theta) \tag{A.2a}$$

$$\eta_1 = B_1^{(p)} R P_1(\cos\Theta) \tag{A.2b}$$

$$\chi_2 = A_3^{(p)} R^2 P_2(\cos\Theta) + A_5^{(p)} R_i^{-2} R^4 P_4(\cos\Theta) + A_7^{(p)} R_i^{-4} R^6 P_6(\cos\Theta) \tag{A.2c}$$

$$\eta_2 = B_2^{(p)} R P_1(\cos\Theta) + B_4^{(p)} R_i^{-2} R^3 P_3(\cos\Theta) + B_6^{(p)} R_i^{-4} R^5 P_5(\cos\Theta) \tag{A.2d}$$

where the Papkovich-Neuber vectors are $\boldsymbol{b}_1 = \eta_1 \mathbf{d}_Z$ and $\boldsymbol{b}_2 = \eta_2 \mathbf{d}_Z$; $P_n(\cos\Theta)$ is the zonal spherical harmonic of degree n and F_0, A_2 etc. are coefficients to be determined by the boundary conditions. The particular solution has the form

$$\boldsymbol{u}_2' = \frac{1}{2\mu}\nabla\zeta - \frac{2(1-\nu)}{\mu}\nabla^2\boldsymbol{w} + \frac{1}{\mu}\nabla\mathrm{Div}\,\boldsymbol{w}$$

where ζ and $\boldsymbol{w}$ depend on the coefficients in eqs. (A.1) and (A.2), and are presented in full in [34].

Appendix B. Far-field stress and displacement

The coefficients in the far-field part of the displacement $\widetilde{\boldsymbol{u}}_{\boldsymbol{w}}$ in eq. (16d), are

$$a_1 = a_{1,1} B_1 G_1 + (a_{1,2} F_0 + a_{1,3} G_1)[3A_2 - 2(1-2\nu_m)]B_1 \tag{B.1a}$$

$$a_2 = -\frac{3R_i^3(\lambda_m + 3\mu_m + 2m_m)}{14\mu_m^2(\lambda_m + 2\mu_m)}[3A_2 - 2(1-2\nu_m)B_1]G_1 \tag{B.1b}$$

where

$$a_{1,1} = -\frac{2(\lambda_m+\mu_m)(3\lambda_m+2\mu_m) - 12\mu_m l_m + 2(3\lambda_m+2\mu_m)m_m - (\lambda_m+2\mu_m)n_m}{24\mu_m^2(\lambda_m+\mu_m)(\lambda_m+2\mu_m)} \tag{B.2a}$$

$$a_{1,2} = -\frac{(\lambda_m+3\mu_m+2m_m)(\lambda_m+\mu_m)}{16\mu_m^2(\lambda_m+2\mu_m)} \tag{B.2b}$$

$$a_{1,3} = -\frac{27\lambda_m^2 + 112\lambda_m\mu_m + 121\mu_m^2 + (54\lambda_m+118\mu_m)m_m - 7(\lambda_m+2\mu_m)n_m}{336\mu_m^3(\lambda_m+2\mu_m)}. \tag{B.2c}$$

The far-field stress $\widetilde{\boldsymbol{P}}'(\boldsymbol{u}_1)$ in eq. (17) may be derived as the order R^{-3} part of the expression $\boldsymbol{P}'(\boldsymbol{u}_1)$, [65, Ch. 9, Eq. (5.1.14)],

$$\boldsymbol{P}'(\mathbf{u}_1) = \boldsymbol{P}^{(1)}\mathrm{Grad}\,\boldsymbol{u}_1 + (2m-n)\vartheta\boldsymbol{\varepsilon} + n\boldsymbol{\varepsilon}^2 + \mu\,\mathrm{Grad}\,\boldsymbol{u}_1(\mathrm{Grad}\,\boldsymbol{u}_1)^T + \left[\lambda\boldsymbol{\omega}\cdot\boldsymbol{\omega} + \left(l - m + \tfrac{1}{2}n\right)\vartheta^2 + \tfrac{1}{2}(\lambda + 2m - n)\right]\boldsymbol{G} \tag{B.3}$$

where $\boldsymbol{G}$ is the identity tensor and

$$\boldsymbol{\varepsilon} = \tfrac{1}{2}\mathrm{Grad}\,\boldsymbol{u}_1 + \tfrac{1}{2}(\mathrm{Grad}\,\boldsymbol{u}_1)^T, \quad \vartheta = \mathrm{Div}\,\boldsymbol{u}_1, \quad \boldsymbol{\omega} = \tfrac{1}{2}\mathrm{Curl}\,\boldsymbol{u}_1.$$

Appendix C. Effective property coefficients

The expressions for the effective TOECs derived using the Maxwell methodology, eq. (24), involve the following coefficients:

$$p_1 = 9K_m^2(10\mu_m + 9\mu_p) + 12K_m\mu_m(34\mu_m + 27\mu_p) + (9K_m^2 - 12K_m\mu_m - 20\mu_m^2)(\mu_m(1-f_0) + f_0\mu_p) + 4\mu_m^2(74\mu_m + 91\mu_p) \tag{C.1a}$$

$$p_2 = p_{2,0} + f_0\mu_m(117K_m^2 + 366K_m\mu_m + 289\mu_m^2)(K_p - K_m)(\mu_p - \mu_m) \tag{C.1b}$$

$$p_3 = p_{3,0} + f_0 p_{3,1} + 12f_0^2\mu_m(3K_m + 11\mu_m)(K_p - K_m)(\mu_p - \mu_m)^2 \tag{C.1c}$$

$$p_4 = p_{4,0} - f_0(162K_m^3 + 585K_m^2\mu_m + 804K_m\mu_m^2 + 314\mu_m^3)(\mu_p - \mu_m) \tag{C.1d}$$

$$p_5 = p_{5,0} + f_0 p_{5,1} + 4f_0^2(27K_m^3 + \tfrac{243}{4}K_m^2\mu_m - 216K_m\mu_m^2 - 334\mu_m^3)(\mu_m - \mu_p)^3 \tag{C.1e}$$

where

$$\begin{aligned} p_{2,0} = {} & [5(3K_m + 4\mu_m)^3 - 7\mu_m(3K_m + 4\mu_m)^2](K_p - K_m)(\mu_p - \mu_m) + 9\mu_m^2(24K_m + 25\mu_m)(K_p - K_m)(\mu_p - \mu_m) \\ & + 5K_m(3K_m + 4\mu_m)[(3K_m + 4\mu_m)^2 + 6\mu_m^2](\mu_p - \mu_m) + 60\mu_m^3(3K_m + 4\mu_m)(K_p - K_m) \end{aligned} \tag{C.2a}$$

$$\begin{aligned} p_{3,0} = {} & 36(K_m + 2\mu_m)^2(\mu_p - \mu_m)^2[3K_m + 4\mu_m + 3(K_p - K_m)] + 180\mu_m(K_p - K_m)(K_m + 2\mu_m)(3K_m + 4\mu_m)(\mu_p - \mu_m) \\ & + 15\mu_m(3K_m + 4\mu_m)^2[4(K_m + 2\mu_m)(\mu_p - \mu_m) + 5\mu_m(K_p - K_m)] + 25\mu_m^2(3K_m + 4\mu_m)^3 \end{aligned} \tag{C.2b}$$

$$\begin{aligned} p_{3,1} = {} & 120\mu_m^2(3K_m + 4\mu_m)(K_p - K_m)(\mu_p - \mu_m) + 6(3K_m + 4\mu_m)[(3K_m + 4\mu_m)^2 - 8K_m\mu_m](\mu_p - \mu_m)^2 \\ & + 6[3(3K_m + 4\mu_m)^2 + 2\mu_m(3K_m + 35\mu_m)](K_p - K_m)(\mu_p - \mu_m)^2 \end{aligned} \tag{C.2c}$$

$$\begin{aligned} p_{4,0} = {} & -10\mu_m(3K_m + 4\mu_m)[9K_m^2 + 24K_m\mu_m + 28\mu_m^2] - [10(3K_m + 4\mu_m)^3 + \mu_m(3K_m + 4\mu_m)^2](\mu_p - \mu_m) \\ & - 6\mu_m^2(42K_m + 55\mu_m)(\mu_p - \mu_m) \end{aligned} \tag{C.2d}$$

$$p_{5,0} = 7[\mu_m(9K_m + 8\mu_m) + 6\mu_p(K_m + 2\mu_m)]^3 \tag{C.2e}$$

$$p_{5,1} = 15\mu_m(\mu_p - \mu_m)^2(3K_m + 4\mu_m)\left(63K_m^2 - 48K_m\mu_m - 128\mu_m^2\right) + (\mu_p - \mu_m)^3(1026K_m^3 + 1161K_m^2\mu_m - 3168K_m\mu_m^2 - 3272\mu_m^3). \tag{C.2f}$$

References

[1] K.Z. Markov, Elementary micromechanics of heterogeneous media, in: K. Markov, L. Preziosi (Eds.), Heterogeneous Media - Micromechanics Modeling Methods and Simulations, Birkhäuser Boston, Boston, MA, 2000, pp. 1–162.

[2] J.C. Maxwell, A Treatise on Electricity and Magnetism, vol. 1, 3rd edition, Clarendon Press, Oxford, 1904.

[3] L.N. McCartney, A. Kelly, Maxwell's far-field methodology applied to the prediction of properties of multi-phase isotropic particulate composites, Proc. R. Soc. A, Math. Phys. Eng. Sci. 464 (2090) (2008) 423–446, https://doi.org/10.1098/rspa.2007.0071.

[4] I. Sevostianov, S.G. Mogilevskaya, V.I. Kushch, Maxwell's methodology of estimating effective properties: alive and well, Int. J. Eng. Sci. 140 (2019) 35–88, https://doi.org/10.1016/j.ijengsci.2019.05.001.

[5] R. Landauer, Electrical conductivity in inhomogeneous media, in: AIP Conference Proceedings, vol. 40, AIP, 1978, pp. 2–45.

[6] J.D. Eshelby, Elastic inclusions and inhomogeneities, in: I.N. Sneddon, R. Hill (Eds.), Progress in Solid Mechanics, North-Holland Publishing Company, Amsterdam, 1961, pp. 89–140.

[7] L.N. McCartney, Maxwell's far-field methodology predicting elastic properties of multiphase composites reinforced with aligned transversely isotropic spheroids, Philos. Mag. 90 (31–32) (2010) 4175–4207, https://doi.org/10.1080/14786431003752142.

[8] I. Sevostianov, A. Giraud, Generalization of Maxwell homogenization scheme for elastic material containing inhomogeneities of diverse shape, Int. J. Eng. Sci. 64 (2013) 23–36, https://doi.org/10.1016/j.ijengsci.2012.12.004.

[9] A.S. Sangani, A. Acrivos, Effective conductivity of a periodic array of spheres, Proc. R. Soc. Lond. Ser. A, Math. Phys. Sci. 386 (1791) (1983) 263–275, https://doi.org/10.1098/rspa.1983.0036.

[10] R.T. Bonnecaze, J.F. Brady, A method for determining the effective conductivity of dispersions of particles, Proc. R. Soc. Lond. Ser. A, Math. Phys. Sci. 430 (1879) (1990) 285–313, https://doi.org/10.1098/rspa.1990.0092.

[11] R.G.C. Arridge, The thermal expansion and bulk modulus of composites consisting of arrays of spherical particles in a matrix, with body- or face-centred cubic symmetry, Proc. R. Soc. Lond. Ser. A, Math. Phys. Sci. 438 (1903) (1992) 291–310, https://doi.org/10.1098/rspa.1992.0107.

[12] V.I. Kushch, Elastic fields and effective stiffness tensor of spheroidal particle composite with imperfect interface, Mech. Mater. 124 (2018) 45–54, https://doi.org/10.1016/j.mechmat.2018.06.001.

[13] V.I. Kushch, R. Springhetti, S.V. Shmegera, Effective permittivity of composite elastomer with account of electric conductivity of phases and imperfect interface, Int. J. Eng. Sci. 123 (2018) 51–61, https://doi.org/10.1016/j.ijengsci.2017.11.016.

[14] A.V. Pyatigorets, S.G. Mogilevskaya, Evaluation of effective transverse mechanical properties of transversely isotropic viscoelastic composite materials, J. Compos. Mater. 45 (25) (2011) 2641–2658, https://doi.org/10.1177/0021998311401091.

[15] V. Levin, S. Kanaun, M. Markov, Generalized Maxwell's scheme for homogenization of poroelastic composites, Int. J. Eng. Sci. 61 (2012) 75–86, https://doi.org/10.1016/j.ijengsci.2012.06.011.

[16] R. Rodríguez-Ramos, J. Otero, Y. Espinosa-Almeyda, F. Sabina, V. Levin, Closed-form expressions for the effective properties of piezoelastic composites reinforced with cylindrical fibers by Maxwell scheme, Mech. Mater. 174 (August) (2022) 104452, https://doi.org/10.1016/j.mechmat.2022.104452.

[17] V.I. Kushch, S.G. Mogilevskaya, Anisotropic imperfect interface in elastic particulate composite with initial stress, Math. Mech. Solids 27 (5) (2022) 872–895, https://doi.org/10.1177/10812865211046650.

[18] E. Polyzos, D. Polyzos, D.V. Hemelrijck, L. Pyl, Capturing size effects in effective field methods through the prism of strain gradient elasticity, Mech. Mater. 186 (September) (2023) 104782, https://doi.org/10.1016/j.mechmat.2023.104782.

[19] D.S. Hughes, J.L. Kelly, Second-order elastic deformation of solids, Phys. Rev. 92 (5) (1953) 1145–1149, https://doi.org/10.1103/PhysRev.92.1145.

[20] F.D. Murnaghan, Finite deformations of an elastic solid, Am. J. Math. 59 (2) (1937) 235, https://doi.org/10.2307/2371405.

[21] Y.H. Pao, W. Sachse, H. Fukuoka, Acoustoelasticity and ultrasonic measurements of residual stresses, in: Physical Acoustics, Academic Press, New York, NY, 1984, pp. 61–143.

[22] A.N. Guz', F.G. Makhort, The physical fundamentals of the ultrasonic nondestructive stress analysis of solids, Int. Appl. Mech. 36 (9) (2000) 1119–1149, https://doi.org/10.1023/A:1009442132064.

[23] A. Hikata, F.A. Sewell, C. Elbaum, Generation of ultrasonic second and third harmonics due to dislocations. II, Phys. Rev. 151 (2) (1966) 442–449, https://doi.org/10.1103/PhysRev.151.442.

[24] K.H. Matlack, J.Y. Kim, L.J. Jacobs, J. Qu, Review of second harmonic generation measurement techniques for material state determination in metals, J. Nondestruct. Eval. 34 (1) (2015) 273, https://doi.org/10.1007/s10921-014-0273-5.

[25] V.K. Chillara, C.J. Lissenden, On some aspects of material behavior relating microstructure and ultrasonic higher harmonic generation, Int. J. Eng. Sci. 94 (2015) 59–70, https://doi.org/10.1016/j.ijengsci.2015.04.008.

[26] R. Hill, On constitutive macro-variables for heterogeneous solids at finite strain, Proc. R. Soc. Lond. Ser. A, Math. Phys. Sci. 326 (1565) (1972) 131–147, https://doi.org/10.1098/rspa.1972.0001.

[27] R.W. Ogden, On the overall moduli of non-linear elastic composite materials, J. Mech. Phys. Solids 22 (6) (1974) 541–553, https://doi.org/10.1016/0022-5096(74)90033-7.

[28] P. Ponte Castañeda, The effective mechanical properties of nonlinear isotropic composites, J. Mech. Phys. Solids 39 (1) (1991) 45–71, https://doi.org/10.1016/0022-5096(91)90030-R.

[29] O. Lopez-Pamies, T. Goudarzi, T. Nakamura, The nonlinear elastic response of suspensions of rigid inclusions in rubber: I—an exact result for dilute suspensions, J. Mech. Phys. Solids 61 (1) (2013) 1–18, https://doi.org/10.1016/j.jmps.2012.08.010.

[30] O. Lopez-Pamies, T. Goudarzi, K. Danas, The nonlinear elastic response of suspensions of rigid inclusions in rubber: II—a simple explicit approximation for finite-concentration suspensions, J. Mech. Phys. Solids 61 (1) (2013) 19–37, https://doi.org/10.1016/j.jmps.2012.08.013.

[31] B. Shrimali, V. Lefèvre, O. Lopez-Pamies, A simple explicit homogenization solution for the macroscopic elastic response of isotropic porous elastomers, J. Mech. Phys. Solids 122 (2019) 364–380, https://doi.org/10.1016/j.jmps.2018.09.026.

[32] B. Shrimali, K. Ghosh, O. Lopez-Pamies, The nonlinear viscoelastic response of suspensions of vacuous bubbles in rubber: I — Gaussian rubber with constant viscosity, J. Elast. (nov 2021), https://doi.org/10.1007/s10659-021-09868-y.

[33] A.A. Semenov, Y.M. Beltukov, Nonlinear elastic moduli of composite materials with nonlinear spherical inclusions dispersed in a nonlinear matrix, Int. J. Solids Struct. 191–192 (2020) 333–340, https://doi.org/10.1016/j.ijsolstr.2020.01.016, arXiv:1905.02301.

[34] J. Vidler, A. Kotousov, C.-T. Ng, Effective elastic properties of a weakly nonlinear particulate composite, Int. J. Non-Linear Mech. 141 (January) (2022) 103949, https://doi.org/10.1016/j.ijnonlinmec.2022.103949.

[35] A.V. Belashov, Y.M. Beltukov, O.A. Moskalyuk, I.V. Semenova, Relative variations of nonlinear elastic moduli in polystyrene-based nanocomposites, Polym. Test. 95 (2021) 107132, https://doi.org/10.1016/j.polymertesting.2021.107132, arXiv:2005.01061.

[36] T. Nakamura, O. Lopez-Pamies, A finite element approach to study cavitation instabilities in non-linear elastic solids under general loading conditions, Int. J. Non-Linear Mech. 47 (2) (2012) 331–340, https://doi.org/10.1016/j.ijnonlinmec.2011.07.007.

[37] B. Shrimali, M. Pezzulla, S. Poincloux, P.M. Reis, O. Lopez-Pamies, The remarkable bending properties of perforated plates, J. Mech. Phys. Solids 154 (May) (2021) 104514, https://doi.org/10.1016/j.jmps.2021.104514.
[38] B. Shrimali, W.J. Parnell, O. Lopez-Pamies, A simple explicit model constructed from a homogenization solution for the large-strain mechanical response of elastomeric syntactic foams, Int. J. Non-Linear Mech. 126 (July) (2020) 103548, https://doi.org/10.1016/j.ijnonlinmec.2020.103548.
[39] S. Li, Y. Mao, W. Liu, S. Hou, A highly efficient multi-scale approach of locally refined nonlinear analysis for large composite structures, Compos. Struct. 306 (December 2022) (2023) 116578, https://doi.org/10.1016/j.compstruct.2022.116578.
[40] A. Bensoussan, J.-L. Lions, G. Papanicolaou, Asymptotic Analysis for Periodic Structures, Studies in Mathematics and Its Applications, vol. 5, North-Holland Pub. Co., Amsterdam, 1978.
[41] J. Fish, Z. Yang, Z. Yuan, A second-order reduced asymptotic homogenization approach for nonlinear periodic heterogeneous materials, Int. J. Numer. Methods Eng. 119 (6) (2019) 469–489, https://doi.org/10.1002/nme.6058.
[42] Z. Yang, Y. Sun, Y. Liu, J. Cui, Prediction on nonlinear mechanical performance of random particulate composites by a statistical second-order reduced multiscale approach, Acta Mech. Sin. 37 (4) (2021) 570–588, https://doi.org/10.1007/s10409-020-01025-3.
[43] J.-Y. Kim, A. Bellotti, P. Alapati, K.E. Kurtis, J. Qu, L.J. Jacobs, Use of a non-collinear wave mixing technique to image internal microscale damage in concrete, J. Appl. Phys. 131 (14) (apr 2022), https://doi.org/10.1063/5.0086194.
[44] P. Liu, L. Yang, K. Yi, T. Kundu, H. Sohn, Application of nonlinear ultrasonic analysis for in situ monitoring of metal additive manufacturing, Struct. Health Monit. 22 (3) (2023) 1760–1775, https://doi.org/10.1177/14759217221113447.
[45] C. Truesdell, W. Noll, The non-linear field theories of mechanics, in: S.S. Antman (Ed.), The Non-Linear Field Theories of Mechanics, Springer Berlin Heidelberg, Berlin, Heidelberg, 2004, pp. 1–579.
[46] J.E. Marsden, T.J.R. Hughes, Mathematical Foundations of Elasticity, Dover Publications, New York, 1994.
[47] L. Shen, S. Yi, An effective inclusion model for effective moduli of heterogeneous materials with ellipsoidal inhomogeneities, Int. J. Solids Struct. 38 (32–33) (2001) 5789–5805, https://doi.org/10.1016/S0020-7683(00)00370-X.
[48] V. Kushch, I. Sevostianov, V. Chernobai, Effective conductivity of composite with imperfect contact between elliptic fibers and matrix: Maxwell's homogenization scheme, Int. J. Eng. Sci. 83 (2014) 146–161, https://doi.org/10.1016/j.ijengsci.2014.03.006.
[49] F.D. Murnaghan, Finite Deformation of an Elastic Solid, Applied Mathematics Series, John Wiley & Sons, Inc., New York, 1951.
[50] A.E. Green, W. Zerna, Theoretical Elasticity, 2nd edition, Oxford University Press, Oxford, 1968.
[51] J.R. Barber, Displacement function solutions, in: J.R. Barber (Ed.), Elasticity, Springer Netherlands, Dordrecht, 2010, pp. 321–332.
[52] E.H. Kerner, The elastic and thermo-elastic properties of composite media, Proc. Phys. Soc. B 69 (8) (1956) 808–813, https://doi.org/10.1088/0370-1301/69/8/305.
[53] G.J. Weng, The theoretical connection between Mori-Tanaka's theory and the Hashin-Shtrikman-Walpole bounds, Int. J. Eng. Sci. 28 (11) (1990) 1111–1120, https://doi.org/10.1016/0020-7225(90)90111-U.
[54] J. Vidler, A. Kotousov, C.-T. Ng, Effect of randomly distributed voids on effective linear and nonlinear elastic properties of isotropic materials, Int. J. Solids Struct. 216 (2021) 83–93, https://doi.org/10.1016/j.ijsolstr.2021.01.009.
[55] C. Tekoğlu, J.W. Hutchinson, T. Pardoen, On localization and void coalescence as a precursor to ductile fracture, Philos. Trans. R. Soc. A, Math. Phys. Eng. Sci. 373 (2038) (2015) 20140121, https://doi.org/10.1098/rsta.2014.0121.
[56] A. Vishnu, G. Vadillo, J. Rodríguez-Martínez, Void growth in ductile materials with realistic porous microstructures, Int. J. Plast. 167 (February) (2023) 103655, https://doi.org/10.1016/j.ijplas.2023.103655.
[57] X. Poulain, V. Lefèvre, O. Lopez-Pamies, K. Ravi-Chandar, Damage in elastomers: nucleation and growth of cavities, micro-cracks, and macro-cracks, Int. J. Fract. 205 (1) (2017) 1–21, https://doi.org/10.1007/s10704-016-0176-9.
[58] N. Gupta, S.E. Zeltmann, V.C. Shunmugasamy, D. Pinisetty, Applications of polymer matrix syntactic foams, JOM 66 (2) (2014) 245–254, https://doi.org/10.1007/s11837-013-0796-8.
[59] M. Destrade, R.W. Ogden, On the third- and fourth-order constants of incompressible isotropic elasticity, J. Acoust. Soc. Am. 128 (6) (2010) 3334–3343, https://doi.org/10.1121/1.3505102, arXiv:1301.7448.
[60] Z. Hashin, Large isotropic elastic deformation of composites and porous media, Int. J. Solids Struct. 21 (7) (1985) 711–720, https://doi.org/10.1016/0020-7683(85)90074-5.
[61] H.M. Smallwood, Limiting law of the reinforcement of rubber, J. Appl. Phys. 15 (11) (1944) 758–766, https://doi.org/10.1063/1.1707385.
[62] V.I. Kushch, I. Sevostianov, The "rigorous" Maxwell homogenization scheme in 2D elasticity: effective stiffness tensor of composite with elliptic inhomogeneities, Mech. Mater. 103 (2016) 44–54, https://doi.org/10.1016/j.mechmat.2016.09.006.
[63] S.G. Mogilevskaya, S.L. Crouch, H.K. Stolarski, A. Benusiglio, Equivalent inhomogeneity method for evaluating the effective elastic properties of unidirectional multi-phase composites with surface/interface effects, Int. J. Solids Struct. 47 (3–4) (2010) 407–418, https://doi.org/10.1016/j.ijsolstr.2009.10.007.
[64] A.V. Pyatigorets, J.F. Labuz, S.G. Mogilevskaya, H.K. Stolarski, Novel approach for measuring the effective shear modulus of porous materials, J. Mater. Sci. 45 (4) (2010) 936–945, https://doi.org/10.1007/s10853-009-4023-5.
[65] A.I. Lurie, A. Belyaev, Theory of Elasticity, Foundations of Engineering Mechanics, Springer Berlin Heidelberg, Berlin, Heidelberg, 2005.